A study of anisotropy in the momentum density of $KHCO_3$ using high-resolution Compton scattering

1994 J. Phys.: Condens. Matter 6 8701

(http://iopscience.iop.org/0953-8984/6/42/003)

J. Phys.: Condens. Matter 6 (1994) 8701–8710. Printed in the UK

A study of anisotropy in the momentum density of $KHCO_3$ using high-resolution Compton scattering

B L Ahuja†, C Bellin‡, J Moscovici‡, E Zukowski§, G Loupias‡‖ and M J Cooper†

† Department of Physics, University of Warwick, Coventry CV4 7AL, UK
‡ Laboratoire de Minéralogie-Cristallographie, Université Paris VI et VII, associé CNRS, case 115, 4 place Jussieu, 75252 Paris Cédex 05, France
§ Institute of Physics, Warsaw University Branch, 15-424 Bialystok, Poland
‖ Laboratoire d'Utilisation du Rayonnement Electromagnétique, CNRS-CEA-MEN, bâtiment 209D, Université Paris-Sud, 91405 Orsay Cédex, France

Received 1 March 1994, in final form 6 June 1994

Abstract. We report directional Compton profiles of $KHCO_3$ measured along the $\pi\pi$ direction (parallel to the HCO_3 layers and parallel to the H bonds), the $\pi\sigma$ direction (parallel to the layers and orthogonal to the H bonds), and the $\sigma\sigma$ direction (orthogonal to the layers and orthogonal to the H bonds) using a high-resolution Compton spectrometer at the LURE-DCI synchrotron facility in France operating at 19.9 keV. These measurements confirm the significant anisotropy of the electron distribution in $KHCO_3$, which we associate with the H bonds. This assumption is supported by the fact that the free-atom model (anions HCO_3^- without H bonds) is not able to describe our experimental results. A molecular orbital–LCAO–self-consistent model has been used to calculate the anisotropies with different size clusters, and taking into account or not the environment of the dimeric anion $(HCO_3)_2^{2-}$ containing two H bonds. The calculated anisotropies based on free $K_2(HCO_3)_2$ yield the main features of the experimental anisotropies with respect to the $\pi\pi$ direction. More sophisticated calculations involving $K_4(HCO_3)_4$ and $K_6(HCO_3)_6$ with the dimeric anion $(HCO_3)_2^{2-}$ surrounded by point charges have not improved the agreement with the experiment. Moreover, none of these calculations is able to describe the small measured anisotropy between $\pi\sigma$ and $\sigma\sigma$ directions.

1. Introduction

Potassium hydrogen carbonate, $KHCO_3$, is a favourable system for orientation-dependent studies of hydrogen bonds. The pairs of CO_3 ions are joined by H bonds into cyclic dimers $(HCO_3)_2^{2-}$. These dimers, which are stacked in layers, and the H bonds that hold together the two HCO_3^- monomers in the dimers, are uniformly aligned parallel to one another in the layer structure of the crystal lattice as shown in figure 1. The K^+ ions are situated just above and below these layers [1]. This structure is monoclinic with $a = 15.1725$ Å, $b = 5.2683$ Å, $c = 3.7110$ Å and $\beta = 104.631°$. Due to the unique hydrogen bond direction within the layers it is possible to examine the orientation-dependent contributions to the properties of the total system with least influence from the other bonds in this system.

During the last two decades hydrogen bonding in $KHCO_3$ has been studied by numerous theoretical as well as experimental methods (see, for example, Brauchler *et al* [2], Weber *et al* [3], Tomkinson *et al* [4], Postorino *et al* [5]). The Compton scattering (measurements of the electronic momentum distribution) work by Brauchler *et al* [2], which used a solid-state detector and 60 keV gamma-rays from a ^{241}Am radioisotope, is affected by

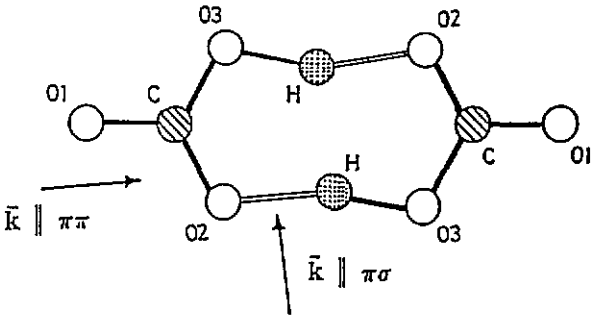

Figure 1. The two-dimensional internal geometry of the $(HCO_3)_2^{2-}$ ions with scattering vector k shown parallel to $\pi\pi$ and $\pi\sigma$ directions. The third direction $\sigma\sigma$ (not shown here) is perpendicular to the plane of the paper and the hydrogen bond.

poorer resolution (0.54 au) than that reported here. These authors have compared their measurements to theoretical $B(z)$ functions based on *ab initio* molecular orbital–LCAO–self-consistent calculations. The work by Weber *et al* [3] is based on optical determination of structural motion while Tomkinson *et al* [4] have discussed vibrational spectroscopy of H bonds in $KHCO_3$. The most recent and interesting work on this complex crystal is by Postorino *et al* [5], who, using deep inelastic neutron scattering (DINS), measured the anisotropy of the proton momentum distribution in $KHCO_3$. They reported a significant difference (about 16%) in the RMS momenta of the proton perpendicular and parallel to the H bonds.

To complete a systematic study on anisotropy in momentum distributions it was considered worthwhile to reinvestigate the electron momentum distribution in $KHCO_3$ using the high-resolution (0.16 au) Compton spectrometer at the Laboratoire pour l'Utilisation du Rayonnement Electromagnetique (LURE-DCI) synchrotron facility at Orsay, France [6, 7]. In this paper we report anisotropies in momentum densities along three physically significant directions, namely (i) the $\pi\pi$ direction (parallel to the layer and parallel to the H bonds), $k = (7.678, 0, 1)$, (ii) the $\pi\sigma$ direction (parallel to the layer and orthogonal to the H bonds), $k = (0, 1, 0)$ and (iii) the $\sigma\sigma$ direction (orthogonal to the layer and orthogonal to the H bonds), $k = (-2.829, 0, 1)$. The vector components are the Miller indices of the planes perpendicular to the scattering vector. These anisotropies are compared with theoretical anisotropies derived from autocorrelation functions based on MO–LCAO–SCF calculations as reported by Brauchler *et al* [2]. These calculations, made taking into account the environment of the dimeric anion $(HCO_3)_2^{2-}$, will be discussed in the last part of this paper.

2. Method

The Compton profile, $J(p_z)$, is the projection of the electron momentum density, $n(\boldsymbol{p})$, along the scattering vector usually chosen as the z axis of a Cartesian coordinate system. Within the impulse approximation (IA), in which the scattering is from individual electrons, the binding energies can be neglected and the final state of the electron is taken as a plane wave. Under these conditions, associated with high energy transfers, $J(p_z)$ is given by [8]

$$J(p_z) = \iint n(\boldsymbol{p})\,\mathrm{d}p_x\,\mathrm{d}p_y \tag{2.1}$$

where $n(\boldsymbol{p})$, the electron momentum density, is related to the electron-momentum and real-space wave functions $\chi(\boldsymbol{p})$ and $\psi(\boldsymbol{r})$ respectively by

$$n(\boldsymbol{p}) = |\chi(\boldsymbol{p})|^2 \left| \int \psi(\boldsymbol{r}) e^{i\boldsymbol{p}\cdot\boldsymbol{r}/\hbar} \, d\boldsymbol{r} \right|^2. \tag{2.2}$$

The connection between the spectrum of the Compton scattered photons and theoretical Compton profiles is through the differential Compton scattering cross-section, which is proportional to $J(p_z)$. The Compton profile is particularly sensitive to the behaviour of the valence electrons in the target, which are well localized in momentum space; it thus provides a basis to test various theoretical electron wave functions. Another important aspect of Compton measurements is that, if one measures the profile of a single crystal with the scattering vector $\boldsymbol{k}$ along various crystallographic directions, then the difference between various profiles reflects the anisotropy of the momentum distribution. Consideration of directional difference profiles minimizes residual systematic errors in the data processing and gives reliable information about bonding in solids and molecules [8]. (Atomic units (au), where $e = \hbar = m = 1$ and $c = 137$ are used in these studies: 1 au of momentum$= 1.993 \times 10^{-24}$ kg m s^{-1}; 1 au in position space$= 0.5289$ Å).

Information concerning the electron distribution can also be obtained in real space from the momentum-space quantity, $J(p_z)$, by Fourier transformation. This quantity, alternatively called the $B(z)$ function, was introduced by Pattison *et al* [9] and is given by

$$B(z) = \int J(p_z) \exp(-ip_z z) \, dp_z = \int \psi^*(\boldsymbol{r} + \boldsymbol{z}) \psi(\boldsymbol{r}) \, d\boldsymbol{r}. \tag{2.3}$$

As defined by (2.3), the $B(z)$ function is also seen to be an autocorrelation function of the one-electron configuration-space wave function along the z axis.

The Compton-scattering data can be analysed in two equivalent ways. The first is by Fourier transformation of the Compton profile to yield $B(z)$ as given in (2.3). This reduces the influence of some systematic errors, in particular multiple scattering in both the target and the source in the γ-ray case. This should be expected since multiple scattering makes a broad and slowly varying contribution to the Compton profile, hence it will make a sharp contribution to $B(z)$ at very low z. In this case the region of chemical interest for the bonding behaviour is at larger values of z (> 3 au). Moreover, the finite resolution is manifest as a multiplicative attenuation of the $B(z)$ function by a position space function that is the Fourier transform of the momentum-space resolution function. It attenuates the signal dramatically at the resolution corresponding to γ-ray experiments. The poorer the momentum resolution, the faster the damping of the $B(z)$ function. For example, in the case of a typical γ-ray experiment [20] with nominal resolution (FWHM) of 0.53 au the autocorrelation distance, z, where the information is damped by a factor of two is as low as 5 au while it is approximately 17 au in our experiment. Noise in the experimental $B(z)$ functions reported by Brauchler *et al* [2] masks its intersections with the z axis and distorts the peak amplitudes of the function, so that their values can only be considered qualitatively.

The second way is to calculate the anisotropy in the directional Compton profiles; the directional difference profiles $J_{hkl}(p_z) - J_{h'k'l'}(p_z)$ are virtually free from systematic errors, both theoretical and experimental. Therefore, in the present work, instead of comparing $B(z)$ functions we have considered anisotropies in momentum densities in terms of Compton profiles below 0–6.2 au of momentum.

3. Experiment

Compton profiles have been measured using a three-axis focusing high-resolution spectrometer at LURE-DCI installed on the wiggler beam time. The positron storage ring, DCI, operates at 1.85 GeV and has critical energy of 3.65 keV. A magnetic superconductor three pole wiggler provides high-energy flux to our experiment: the critial energy is about 8 keV. The synchrotron radiation beam is monochromatized to produce an energy of 19.9 keV by Bragg reflection from a double-crystal 220 Si monochromator. The choice of the incident energy was made to fulfil the IA for as many target electrons as possible subject to the diminishing flux at increasing photon energy. The photons are scattered at an angle of 135° and the entire path of this scattered beam is under vacuum. Their energy was analysed by means of a Si(440) Cauchois curved analysing crystal, focused to a single point on the Rowland circle and detected by a position-sensitive detector, filled with Xe at 4 atm pressure, which is situated tangentially to the Rowland (focal) circle. The analysing crystal was cut in such a way that analyser glitches (for details, see [10]) do not appear in the Compton-profile region for the chosen incident energy. The separation between data points is equivalent to 0.03 au when expressed in terms of the electron-momentum scale. The resolution function is measured from the full width at half maximum of the thermal diffuse scattering (TDS) peak, which is 0.16 au. The TDS peak can be fitted by a Gaussian curve whose standard deviation σ, is 0.07 au of momentum. The $KHCO_3$ single crystals, as used in the work of Tomkinson *et al* [4], had been prepared by slow evaporation of a saturated aqueous solution at room temperature. These crystals were oriented using x-ray diffraction in order to successively align the scattering vector along the $\pi\pi$, $\pi\sigma$ and $\sigma\sigma$ directions to perform each measurement. For each measurement more than one million counts were collected in the region of the Compton profile during 20–24 h when LURE-DCI was running with an average current of 200 mA.

4. Data processing

The weak background, which is about 1% of the Compton signal at the Compton peak and arises mainly from electronic noise, was subtracted out [6, 7]. This was accomplished by fitting the theoretical core profile to the high-momentum data, at $|p_z| \geqslant 6.2$ au (where there is no significant valence contribution), and assuming a linear variation of the background under the Compton line. The core electrons are unaffected by chemical bonding and the calculated atom profiles therefore give a good representation of the core electron behaviour in the crystalline solid. This procedure depends upon the multiple scattering being negligible; evidence for this assumption is presented below.

To compute the total theoretical core profile of $KHCO_3$, we used both the quasi-self-consistent-field (QSCF) method of calculation [11] and the free-atom Compton profiles of Biggs *et al* [12]. The QSCF method is useful for elements where the energy transfer to the target electron is not much higher than its binding energy, i.e. when the IA cannot be assumed to be valid. The details of the QSCF method have been published elsewhere [11].

In the present experimental conditions, the energy (ΔE) transferred to an electron at rest by a 19.9 keV photon, upon scattering through 135°, is 1300 eV and the binding energies of 1s electrons of C and O are 284 eV and 532 eV [13] respectively. For the 1s electrons of C and O we have employed the QSCF method to calculate the core Compton profiles. In slightly heavier elements such as K the supremacy of the QSCF approach is not clear, so we have considered impulse (free-atom) Compton profiles for this element, for which the

energy transfer is more than four times any of the 2s and 2p electron binding energies [12]. Further, since the binding energy [13] of the K shell (3027 eV) of K is higher than ΔE, these electrons do not give any contribution to the spectrum. After the subtraction of the background the data were corrected for sample and analyser absorption, detector efficiency and the energy dependence of the cross-section [6, 7].

Since the K-shell electrons of K do not contribute at all to the Compton profile in the present experiment, the theoretical profiles were normalized to 23.04 electrons. This is the area of the corresponding free-atom profile in the momentum range of up to 6.2 au excluding entirely the contribution of K 1s electrons and allowing for the binding energies of other electrons.

Due to changes in photon polarization after the first and second inelastic collisions, and in transmission through the analysing crystal, the multiple scattering is negligible [14]. For example, in an earlier paper on the multiple-scattering correction for Be in the geometry of the Compton spectrometer at LURE-DCI, Chomilier *et al* [14] concluded that the effect of double scattering by low-energy, linearly polarized, synchrotron radiation at $J(0)$ is only about 30% of the double scattering by unpolarized photons. In the Be case the ratio of the total number of doubly to singly scattered photons was 0.03 for a sample thickness (3 mm) large enough to yield 70% absorption. It has been concluded by several workers [15–18] that when the photoelectric absorption is total for the available thicknesses, the ratio of multiple to single scattering saturates, as was demonstrated in Monte Carlo simulation. For $KHCO_3$ samples, the thickness was sufficient for the absorption to be always more than 98.7%, in respect with the orientation of the sample (the angle between the incident beam and the sample). For the $\pi\pi$, $\pi\sigma$ and $\sigma\sigma$ directions, measurements have been performed respectively with samples of thicknesses of 4 mm, 2.72 mm and 1.36 mm. Therefore the small saturated multiple scattering is, to a very good approximation, the same in each directional profile it subtracts from the directional difference profiles; therefore we have not corrected our directional difference profiles for the effect of multiple scattering. All the valence profiles (total profile−core profile), are normalized in the momentum range 0–6.2 au to 12 electrons, which is half the valence number of electrons in the compound studied.

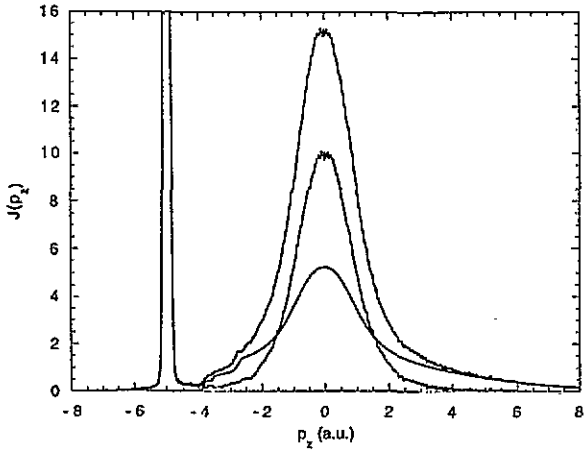

Figure 2. The symmetrized corrected total experimental Compton profile (top), symmetrized valence Compton profile (middle) and theoretical core Compton profile (bottom) of $KHCO_3$ for the $\pi\pi$ direction. The sharp peak on the left-hand side is the elastic line. The momentum scale is in atomic units of electron momentum.

5. Results and discussion

Figure 2 shows the Compton-profile data together with the calculated core and valence Compton profiles for the $\pi\pi$ direction in momentum space. The data were accumulated in about 20 h of beam time. The edges at $p_z = -3.83$, -3.77 and -2.85 au are due to C (K-shell), K (L-shell) and O (K-shell) core electrons. These edges occur at those values of electron momentum corresponding to an energy transfer equal to the electron-binding energy, i.e. respectively 283, 297 and 532 eV. At an energy transfer close to the binding energy, the description of the core is not good enough to allow us to use the values of $J(q)$ in the range of -3.83 au $< q < -2.16$ au. Within the statistical accuracy, each profile is symmetric around $q = 0$ up to $+2.16$ au. As a consequence, the experimental valence profiles are symmetrized around zero only up to $q = \pm 2.16$ au, leading to a reduction of the error bars by a factor of $\sqrt{2}$.

Table 1. Valence experimental Compton profiles for $\pi\pi$, $\pi\sigma$ and $\sigma\sigma$ directions. Statistical errors are shown at a few points. The profiles are normalized to an area of 12 electrons in the range $0 \leqslant p_z \leqslant 6.2$ au.

p_z (au)	$\pi\pi$ direction	$\pi\sigma$ direction	$\sigma\sigma$ direction
0.00	10.164 ± 0.044	9.968 ± 0.041	9.837 ± 0.041
0.10	10.148	10.008	9.825
0.20	10.043	9.958	9.738
0.30	10.038	9.628	0.487
0.40	9.310	9.117	9.057
0.50	8.764	8.569	8.526
0.60	8.115	7.962	7.951
0.70	7.382	7.284	7.317
0.80	6.668	6.593	6.621
0.90	6.034	5.888	5.916
1.00	5.410 ± 0.039	5.158 ± 0.032	5.231 ± 0.030
1.20	4.016	3.869	3.874
1.40	2.886	2.860	2.872
1.60	1.940	2.149	2.156
1.80	1.413	2.149	1.573
2.00	1.035	1.177	1.218
2.16	0.856 ± 0.016	0.960 ± 0.015	0.956 ± 0.015
2.18[a]	0.841 ± 0.023	0.955 ± 0.021	0.928 ± 0.022
2.40	0.620	0.785	0.735
2.60	0.505	0.616	0.586
2.80	0.432	0.528	0.521
3.00	0.353 ± 0.018	0.411 ± 0.018	0.376 ± 0.018
3.50	0.183	0.217	0.270
4.00	0.119 ± 0.013	0.100 ± 0.014	0.131 ± 0.012
5.00	0.034	0.034	0.032

[a] From $q = 2.16$ au, directional profiles are no longer symmetrized.

Above 6.2 au, our core profile matches completely the total experimental profile, confirming that there is no valence contribution above 6.2 au. The valence data, corrected for all systematic effects except multiple scattering for $\pi\pi$, $\pi\sigma$ and $\sigma\sigma$ directions, are given in table 1. The experimental errors, calculated in the range of momentum equivalent to the FWHM of the instrumental function (0.16 au) are also given at some points.

In figures 3 and 4 the experimental anisotropies of the present data, along with theoretical anisotropies (as explained later), are shown. It is seen that the experimental anisotropies

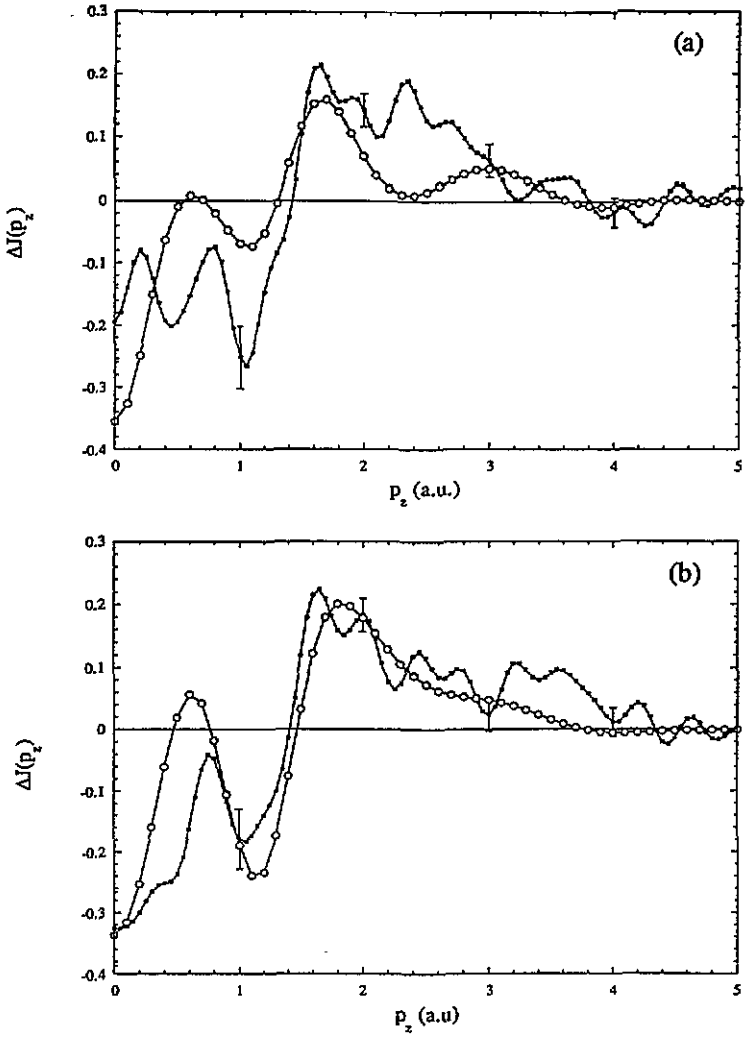

Figure 3. The experimental anisotropies ΔJ (■—■—■) along with the theoretical anisotropies (○—○—○) (a) between $\pi\sigma$ and $\pi\pi$, corresponding to free $K_2(HCO_3)_2$ and (b) between $\sigma\sigma$ and $\pi\pi$, corresponding to $K_4(HCO_3)_4$ within its environment. Error bars are shown at a few points.

with respect to the $\pi\pi$ direction, (figures 3(a) and (b)) have the same main features and are within the statistical noise of the measurements. Between $\pi\sigma$ and $\sigma\sigma$ directions (figure 4) the overall changes in the momentum densities, as evidenced by their Compton profiles, are small.

Brauchler *et al* [2] have determined, using MO–LCAO–SCF calculations, the $B(z)$ functions for increased size of clusters, from $KHCO_3$ up to $K_6(HCO_3)_6$, surrounded or not by point charges. In order to compare with our experimental results, we have shown in figures 3 and 4 the 'best-fit' theoretical anisotropies, chosen by χ^2 fitting between experimental and theoretical anisotropies. This 'best fit' was found for calculations made

(i) for free $K_2(HCO_3)_2$ with the dimeric anion $(HCO_3)_2^{2-}$ containing the H bonds and

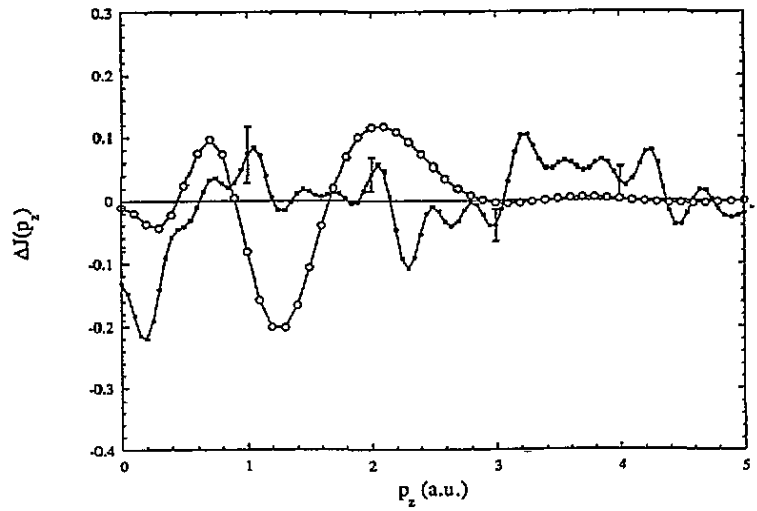

Figure 4. The experimental anisotropy ΔJ (■—■—■) along with the theoretical anisotropy (○—○—○) between $\sigma\sigma$ and $\pi\sigma$, corresponding to free $K_6(HCO_3)_6$. Error bars are shown at a few points.

the orbital contribution of the 32 MOs (figure 3(a)),

(ii) for $K_4(HCO_3)_4$ by orthogonalization of the MOs of two dimeric anions $(HCO_3)_2^{2-}$ surrounded by point charges (figure 3(b)) and

(iii) for free $K_6(HCO_3)_6$ by orthogonalization of the MOs of three dimeric anions $(HCO_3)_2^{2-}$ (figure 4).

However, we have noted that there are no significant differences between all theoretical anisotropies (except, as was said in the introduction, the free-atom case), with respect to the same directions. Moreover, the inclusion of point charges to single or double dimeric anions does not affect significantly the anisotropies in momentum densities. The theoretical Compton profiles have been convoluted with a Gaussian of FWHM = 0.16 au, to mimic the experimental resolution.

In the case of anisotropies with respect to the $\pi\pi$ direction, both theoretical and experimental anisotropies show the same trend near the Compton peak (0–0.2 au). The trend between theoretical and experimental anisotropies is reversed between 0.3 and 0.5 au. For larger momentum the same behaviour is found. The anisotropy in $\sigma\sigma - \pi\pi$ difference (figure 3(b)) is described better by the theoretical calculations than for $\pi\sigma - \pi\pi$ (figure 3(a)). Particularly, near 0.2 au, a first structure appears clearly in $\pi\sigma - \pi\pi$ experimental anisotropy, which is not so evident in $\sigma\sigma - \pi\pi$ experimental anisotropy. Figure 4 also shows the anisotropy between the $\pi\sigma$ and $\sigma\sigma$ directions based on data set 3 (three dimieric anions without point charges), which was found to be in better agreement with the small experimental anisotropies found. As can be seen from this figure, the experimental anisotropy is almost all within statistical noise and much less than the theoretical one: even the best theoretical data set is not in reasonable agreement with experimental results.

The anisotropies with respect to the $\pi\pi$ direction can also be understood in terms of a bond-directional (BD) principle as follows: figure 3(a) and (b) clearly shows that between 0 and 1.5 au the experimental Compton profile values for the $\pi\pi$ direction are higher than for the $\pi\sigma$ and $\sigma\sigma$ directions and after that the opposite trend is followed. This suggests

that, in the case of $KHCO_3$, there is a greater momentum density at low momentum along the H bond ($\pi\pi$ direction) and greater density at high momentum orthogonal to the H bond than was the case in the isolated molecules. This can be explained by the following factors: two major changes occur when the two molecules of HCO_3^- come together to form a bond. First the atomic orbital of H contracts, which, by the Fourier transform principle [8], has the effect of expanding the momentum density in all directions. Secondly, some H electron density is transferred to the region between the two O nuclei. The positive anisotropies at momenta above 1.5 au for $\pi\pi - \pi\sigma$ and $\pi\pi - \sigma\sigma$ directional differences are well explained by the bond-oscillation principle [8], which states that the momentum distribution and Compton profiles associated with the chemical bonds will exhibit oscillations along the bonding direction with a period roughly equal to 2π divided by the bond length. In our case this distance is equal to 1.55 au, which is in agreement with the oscillation found in the present anisotropies.

Now we compare our results with the earlier experimental investigations. For the $\pi\sigma$ and $\sigma\sigma$ directions, as expected, Brauchler *et al* [2] also found very little difference between reciprocal form factors with the dimer, monomer and orthogonalized monomers (the latter were not available to us for comparison). Due to noise in their experimental reciprocal form factors along these directions, the comparisons between theoretical and experimental $B(z)$ functions were not conclusive. In the case of the $\pi\pi$ direction the agreement between theoretical and noisy experimental $B(z)$ function is poor. For the $\pi\pi$ direction they suggested the association of two HCO_3^- anions through the H bonds to the dimeric anion $(HCO_3)_2^{2-}$. We cannot directly compare our experiment with the investigations of Brauchler *et al* [2] due to noise in their experimental $B(z)$ functions and the non-availability of their experimental Compton profiles of $KHCO_3$.

It is worth mentioning here that precise measurements of Compton profiles require both high statistical accuracy and high resolution in momentum. In our measurements the statistical accuracy is only just sufficient. It can be further improved if more beam time is available or if a higher-brightness source is used. The 6 GeV ESRF storage ring, where the spectral flux is of the order of 10^{14} ph s^{-1}/0.1% bandwidth $mrad^{-1}$ up to 10 keV in comparison to 2×10^{12} ph s^{-1}/0.1% bandwidth $mrad^{-1}$ LURE-DCI, could lead to a significant improvement in statistical accuracy and a simultaneous reduction in the measurement time. Furthermore the higher incident photon energies available will facilitate the study of high-Z materials because of lower photoelectric absorption.

However, even with a just sufficient statistical accuracy, we have pointed out the fact that experimental anisotropies are not well described at small momenta whatever the considered directions. Moreover, for medium values of momentum, we have seen that the measured anisotropy in directions perpendicular to the layer (i.e. $\pi\sigma$ and $\sigma\sigma$, figure 4) is lower than the calculated anisotropy, probably due to a solid-state effect not adequately taken into account in the model. To conclude, a more accurate model is needed to describe all features given by the experiment.

Acknowledgments

This work was sponsored by the British Council and French Foreign Ministries under the Alliance programme and by the UK Science and Engineering Research Council. One of us (BLA) is thankful to the Department of Science and Technology, Government of India, New Delhi for a Boyscast fellowship to visit the UK. We are also very thankful to Professor W Weyrich for sending numerical values of the theoretical $B(r)$ functions of $KHCO_3$, and Dr J Tomkinson for the loan of the single crystals used in this work.

References

[1] Thomas J O, Tellgren R and Olovsson I 1974 *Acta Crystallogr.* B **30** 1155, 2540
[2] Brauchler M, Lunell S, Olovsson I and Weyrich W 1989 *Int. J. Quantum Chem.* **35** 895
[3] Weber H J, Schulz M, Schmitz S, Granzin J and Siegert H 1989 *J. Phys.: Condens. Matter* **I** 8543
[4] Tomkinson J, Kearley G J and Fillaux F 1991 *Physica* B **174** 246
[5] Postorino P, Fillaux F, Mayers J, Tomkinson J and Holt R S 1991 *J. Chem. Phys.* **94** 4411
[6] Loupias G and Petiau J 1980 *J. Physique* **41** 265 and references therein
[7] Loupias G, Petiau J, Issolah A and Schneider M 1980 *Phys. Status Solidi* B **102** 79 and references therein
[8] Cooper M J 1985 *Rep. Prog. Phys.* **48** 415
B Williams (ed) 1977 *Compton Scattering* (London: McGraw-Hill)
[9] Pattison P, Weyrich W and Williams B 1977 *Solid State Commun.* **21** 967
[10] Lann G V D and Thole B T 1988 *Nucl. Instrum. Methods* A **263** 515
[11] Issolah A, Garreau Y, Lévy B and Loupias G 1991 *Phys. Rev.* B **44** 11029
Issolah A, Lévy B, Beswick A and Loupias G 1988 *Phys. Rev.* A **38** 4509
[12] Biggs F, Mendelsohn L B and Mann J B 1975 *At. Nucl. Data Tables* **16** 201
[13] Beardeen J A and Burr A R 1967 *Rev. Mod. Phys.* **39** 125
[14] Chomilier J, Loupias G and Felsteiner J 1985 *Nucl. Instrum. Methods* A **235** 603
[15] Williams B G and Halonen V 1975 *Phys. Fennica* **10** 5
[16] Halonen V, Williams B and Paakkari T 1975 *Phys. Fennica* **10** 107
[17] Felsteiner J and Pattison P 1975 *Nucl. Instrum. Methods* **124** 449
[18] Pitkanen T, Cooper M J, Laundy D and Holt R S 1987 *Nucl. Instrum. Methods* A **257** 384
[19] Weyrich W 1992 private communication
[20] Pattison P and Weyrich W 1979 *J. Phys. Chem. Solids* **40** 213